A continental-scale approach to ecosystem condition monitoring using satellite imagery and deep learning

Christopher Owers, Karel Mokany, Chris Ware, Thomas Harwood, Jinyan Yang, Randall Donohue, Tim Mcvicar, Eric Lehmann, Kristen Willams, Rebecca Schmidt, et al.

Ecological Informatics 94 (2026) 103639

Contents lists available at ScienceDirect

Ecological Informatics

journal homepage: www.elsevier.com/locate/ecolinf

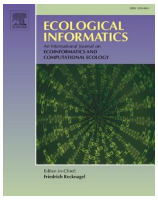

A continental-scale approach to ecosystem condition monitoring using satellite imagery and deep learning

Christopher J. Owers [a,b,*], Karel Mokany [b], Chris Ware [c], Thomas D. Harwood [b,d], Jinyan Yang [b], Randall J. Donohue [b], Tim R. McVicar [b], Eric A. Lehmann [e], Kristen J. Willams [b], Rebecca K. Schmidt [b], Matt Paget [b], Simon Ferrier [b], Charlotte Pelletier [f]

[a] Earth Sciences, School of Science, University of Newcastle, Callaghan, NSW, Australia
[b] CSIRO, Canberra, ACT, Australia
[c] CSIRO, Sandy Bay, TAS, Australia
[d] Environmental Change Institute, School of Geography and the Environment, University of Oxford, Oxford, UK
[e] Data61, CSIRO, Canberra, ACT, Australia
[f] Université Bretagne Sud, Institute for Research in IT and Random Systems (IRISA), Institut Universitaire de France (IUF), Vannes, France

ARTICLE INFO

Keywords:
Habitat condition
Biodiversity
Convolutional neutral networks
CNNs
Remote sensing
Landsat
Australia

ABSTRACT

Substantial declines in biodiversity over the past century demonstrate an immediate need to preserve ecosystems and further mitigate habitat loss. Monitoring changes in ecosystem condition at region thru continental to global scales can provide important information about biodiversity declines and help facilitate targeted intervention. Efforts to use satellite imagery to map ecosystem condition change have experienced challenges with distinguishing observed changes from the natural variation of ecosystems. In this study we use an innovative deep learning architecture to pair time series satellite imagery with locations of known on-ground condition. Our model was developed using 209,041 on-ground records of native species present in the landscape, as a surrogate measure of ecosystem condition, coupled with Landsat time series data and topographic and climatological datasets. We predict ecosystem condition across the Australian continent for several years (2010, 2015, 2020, 2021, 2022) at 100 m. Arid regions in Australia's interior had predicted condition scores close to reference condition (1) for all years. Comparatively, highly modified landscapes in Australia's southeastern and southwestern regions had predicted condition scores closer to fully degraded (0). Mean predicted ecosystem condition across Australia was greater than 0.65 for all years, suggesting greater overall presence of native species rather than absence, however this was spatially variable. Our results demonstrate that using deep learning techniques and time series data can provide quantitative information on ecosystem condition, accounting for temporal variability of vegetation phenology and spatial variability across bioregions. Ongoing efforts to collect essential biodiversity variables from space must consider integrating with deep leaning approaches that have capacity for context driven spatial modelling. This will help ensure mapping products can support policy and inform intervention strategies.

1. Introduction

Global declines in biodiversity have been observed over the past century and are directly linked to sustained anthropogenic pressures on ecosystems (Ceballos et al., 2015; Díaz and Malhi, 2022; Jaureguiberry et al., 2022; Johnson et al., 2017). Biodiversity is important for ecosystem function, providing key ecosystem services for society (IPBES, 2019). There is an immediate need to reduce losses in biodiversity and preserve existing biodiverse landscapes, particularly given projected changes in the global climate (Loreau et al., 2022; Pereira et al., 2024). Losses in biodiversity are often linked with landscape change and reduction in suitable habitat extent (Hooper et al., 2012; Jaureguiberry et al., 2022). These losses in suitable habitat can occur at varying spatial and temporal scales, from smaller acute ecosystem extent loss to larger slow degradation of ecosystem condition (Krauss et al., 2010; Watson et al., 2016).

* Corresponding author at: Earth Sciences, School of Science, University of Newcastle, Callaghan, NSW, Australia.
E-mail address: chris.owers@newcastle.edu.au (C.J. Owers).

https://doi.org/10.1016/j.ecoinf.2026.103639
Received 21 July 2025; Received in revised form 24 November 2025; Accepted 1 February 2026
Available online 5 February 2026

Changes in ecosystem condition are linked to habitat loss and quality of habitat for biodiversity (Chase et al., 2020; Hooper et al., 2012). The condition of an ecosystem can provide an important indicator of changes that manifest in global biodiversity declines (Chase et al., 2020). Monitoring changes in ecosystem condition can also inform identification of drivers and pressures on ecosystems to understand the response of biodiversity in landscapes (McNellie et al., 2020; Nicholson et al., 2021). Ecosystem condition can be defined as the structure, function and composition of a given instance of an ecosystem relative to that expected if the ecosystem were in reference condition (Nicholson et al., 2021; SEEA-EA, 2024). However, the interpretation of characteristics such as structure, function and composition, as well as ecosystem reference states requires a clear framework to enable identification of ecosystem condition change (McNellie et al., 2020).

Measuring ecosystem condition and identifying changes in ecosystem condition over time requires a clear definition of 'condition' (Tierney et al., 2009; Wurtzebach and Schultz, 2016). Measures of key characteristics of ecosystems such as structure, function or composition are often used as proxies for ecosystem condition (McNellie et al., 2020; Nicholson et al., 2021). Ground-based measures, such as vegetation plots or transects, are very useful for site specific indicators of ecosystem condition (Tierney et al., 2009; Yen et al., 2019). Repeated measures at these locations can provide high confidence of identifying changes over time (Karan et al., 2016). However, ground-based measures are usually resource intensive to collect, particularly in remote locations which are often most valuable for identifying long term ecosystem condition change with limited acute anthropogenic pressures. Broad scale approaches, such as those derived from remote sensing, are also valuable to provide consistent spatial and temporal snapshots of ecosystem condition and its change over time retrospectively, where no on-ground data are available (Harwood et al., 2016; Williams et al., 2024).

Mapping ecosystem condition over regional thru continental to global scales has been achieved using a variety of data sources (McFarlane and Wallace, 2019; Nagendra et al., 2013). Approaches using land cover (Venter et al., 2022), land use (Gomes et al., 2021), or anthropogenic impact such as human footprint or night-time lights (Venter et al., 2016; Zhao et al., 2019) have been used as a proxy for identifying ecosystem condition change. However, these approaches often rely on inference of human pressures to ecosystem condition change rather than direct observations of ecosystem state. Earth Observation (EO) data such as satellite imagery have been used to provide observations of ecosystem condition change over such large spatial extents, with the capacity to provide high temporal frequency of change (Hansen et al., 2021; Pelletier et al., 2019). Approaches to mapping ecosystem condition using EO have developed relationships of observations to locations in known reference condition (e.g. Habitat Condition Assessment System (HCAS) (Harwood et al., 2016; Valavi et al., 2025; Williams et al., 2024)). Due to the complexity of the relationships between ecosystem condition, vegetation attributes and environmental covariates, machine learning algorithms to identify pixels in reference condition or degraded states has also been demonstrated (Kocev et al., 2009; Lawley et al., 2016; Love et al., 2020; McNellie et al., 2021). These approaches highlight the challenges of identifying changes in ecosystem condition over space and time, such as bioregional variation in ecosystem states within and between bioregions and vegetation phenology. Distinguishing observed changes in ecosystem condition from the natural variation of ecosystems using EO data requires new approaches that can integrate information on the spatial and temporal context of observed change.

Deep learning may offer a useful approach to overcoming challenges in mapping and monitoring ecosystem condition from EO data. Deep learning techniques can accommodate data from different modalities, at various scales, and across multiple geographical regions, while maintaining good generalisation performance. For example, convolutional neural networks (CNNs) are a type of deep learning model that use multiple convolutional layers to learn and represent complex patterns in data (O'Shea and Nash, 2015). CNNs are particularly useful as they have the capacity to use data in the context of other data, such as image interpretation (Chauhan et al., 2018). In computer vision tasks, a convolutional operation involves moving a kernel filter over the input image to obtain a new representation of the data that should be relevant for classification. These techniques have translated to remote sensing applications, providing contextual data to classification of satellite images (Zhang et al., 2021; Zhu et al., 2017). CNNs may be well suited to the challenges of modelling and mapping ecosystem condition as they can consider complex interactions between variables, adjusting for the complexities of environmental context thereby estimating ecosystem condition.

A time series CNN architecture was proposed for EO by Pelletier et al. (2019) and has been used in a variety of applications for identifying land cover (Lucas et al., 2021), land use (Wang et al., 2021) and fuel moisture content (Miller et al., 2022; Zhu et al., 2021). This approach utilises the contextual information of a pixel's time series observations to determine classification or estimation outputs. Similar deep learning workflows have demonstrated capacity to accommodate the temporal aspect of seasonality for vegetation phenology (Miller et al., 2024). Indeed, these workflows have demonstrated to provide greater accuracy than more traditional machine learning algorithms such as Random Forest and Support Vector Machine (Miller et al., 2024; Pelletier et al., 2019). Moreover, recent CNN approaches have incorporated geographical context through input layers of soil, climate, geology and land use (Miller et al., 2023). This provides greater generalisation of deep learning models across wide geographic extents to examine a pixel's time series observations in context of environmental conditions. To enable approaches using EO data that capture changes in ecosystem condition over time we need to capture phenological and environmental variation within the context of the broader landscape.

The aim of this study was to develop a consistent and continent-wide ecosystem condition mapping approach using EO data and innovative deep learning techniques. More specifically, we mapped the proportion of native species present in the landscape as a surrogate measure of ecosystem condition at 100 m resolution utilising the Landsat imagery archive for Australia and its territories. We use a deep learning architecture to pair time series EO information with locations of known on-ground condition, accounting for spatiotemporal variation of vegetation. We focus on evaluating this approach for delineating observed changes in ecosystem condition from the natural variation of ecosystems by generating several annual maps (2010, 2015, 2020, 2021, 2022).

2. Methods

2.1. Study area

The focus of this study was the Australian continent, which spans 7.7 million km^2 with a latitudinal range from 10°41′ S to 43°38′ S. Australia encompasses six major climate groups (Beck et al., 2018, 2023), including tropical regions in the north, extensive arid areas inland, and temperate zones in the south. Despite only 18% of the land being desert, up to 70% of the mainland receives less than 500 mm of rainfall annually, varying greatly with elevation, latitude, and interannual climate fluctuations such as El Niño–Southern Oscillation. Australia exhibits complex and varying landscapes, with over 80 distinct bioregions supporting a range of ecosystem types (National Land and Water Resources Audit, 2001). Reported changes in ecosystem condition across Australia include a continual trend of native vegetation removal for agriculture and urban expansion (Cresswell et al., 2021; Harwood et al., 2016; White et al., 2020) as well as climate impacts on vegetation cover and productivity (Donohue et al., 2009; Lamchin et al., 2020; Xie et al., 2019).

The deep learning model presented in this paper was developed using over 30 years of on-ground data (Mokany et al., 2022) coupled with the Landsat imagery archive (Wulder et al., 2016). Five calendar

years (2010, 2015, 2020, 2021, 2022) were selected to apply and evaluate the proposed approach for continental scale ecosystem condition mapping. These years represent the range of climatic conditions common to the Australian continent; 2010 was one of the wettest years on record (records commenced in 1900) with mean rainfall well above the long-term average (2010, 690 mm yr^{-1}; 1961–1990 average, 465 mm yr^{-1}) with this attributed to a significant La Niña event (BOM, 2012). 2015 represented a particularly warm and dry year, with mean temperatures 0.83 °C above the 1961–1990 average, coinciding with below average rainfall (2015, 444 mm yr^{-1}; BOM (2016). Three recent years (2020,2021,2022) were also selected to apply and evaluate this approach for demonstration of temporal and spatial consistency of proportion native species predictions as a surrogate measure of ecosystem condition across the continent.

2.2. Data

2.2.1. Ground data

Input data to the deep learning model consisted of information on the proportion of native species present in the landscape and was collated from a variety of sources and timespans. For the purpose of this study, systematically collected vegetation plot data were used as the basis for estimating a binary measure of intact or degraded natural systems for training. It was assumed that all plots where proportion of native species recorded was greater than 90% likely constituted a condition score at or near reference (1), and a complete absence of these species indicating a likely condition score of degraded (0) (Fig. 1). Whilst it is possible that plots could lose a large number of native species due to habitat degradation without non-native species being introduced, this was assumed to be a rare case. Ecosystem condition input data at or near reference were obtained using the harmonised Australia vegetated plot (HAVPlot) dataset (Mokany et al., 2022).

Further input data considered as fully degraded condition (0) were obtained by using features such as roads, parking lots and buildings from Open Street Map (OpenStreetMap contributors, 2017), plantation and vineyard locations (AARSC, 2021; ABARES, 2021), cultivated areas (Owers et al., 2022), and where HAVPlot data indicated less than 10% proportion of native species (Mokany et al., 2022). A selection of input data considered as degraded were subsampled through random stratification based on Köppen major climate groups to facilitate spatial representativeness across Australia and at least match proportionally the input data with a condition score of 1 (i.e. at least same number of records for full degraded condition as at or near reference selected per major climate group). Minor additional input data were generated with expert interpretation for areas of very low representativeness. There were 209,041 records with a location, date and ecosystem condition score input to the deep learning model (fully degraded condition = 138,483; at or near reference = 70,558).

2.2.2. Earth observation data

Earth observation (EO) data were accessed using the CSIRO Earth Analytics Science and Innovation (EASI) platform. EASI builds upon the Open Data Cube framework to store, access and analyse EO data using cloud computing services (Woodcock et al., 2018). For this study, the Landsat archive was accessed through EASI in analysis-ready format (Dhu et al., 2017; Lewis et al., 2017) combining Landsat 5, 7 and 8 data where available. To enable consistent analysis over space and through time, Landsat data were pre-processed to surface reflectance and adjusted for solar angle, terrain illumination, as well as removal of cloud and cloud shadow (Byrne et al., 2024; Lewis et al., 2017; Li et al., 2012; Zhu and Woodcock, 2012). Spectral reflectance values of 6 reflectance bands (Blue, Green, Red, NIR, SWIR1, SWIR2) were extracted for each observation in specified calendar years and 17 common spectral indices were generated relevant for landscape and vegetation characteristics relating to ecosystem condition (NDVI, EVI, LAI, SAVI, MSAVI, TCG, NDWI, MNDWI, TCW, BUI, NBI, NDBI, TCB, BAI, NBR, BSI, NDMI; see Table S1). Additional nationally available spatial data layers were also used to provide topographical and climatological context. These included a digital elevation model (Farr et al., 2007) and topographic wetness index (Gallant and Austin, 2015), latitude and longitude, as well as climatology datasets including mean annual potential evaporation, mean annual precipitation, mean maximum temperature of the warmest

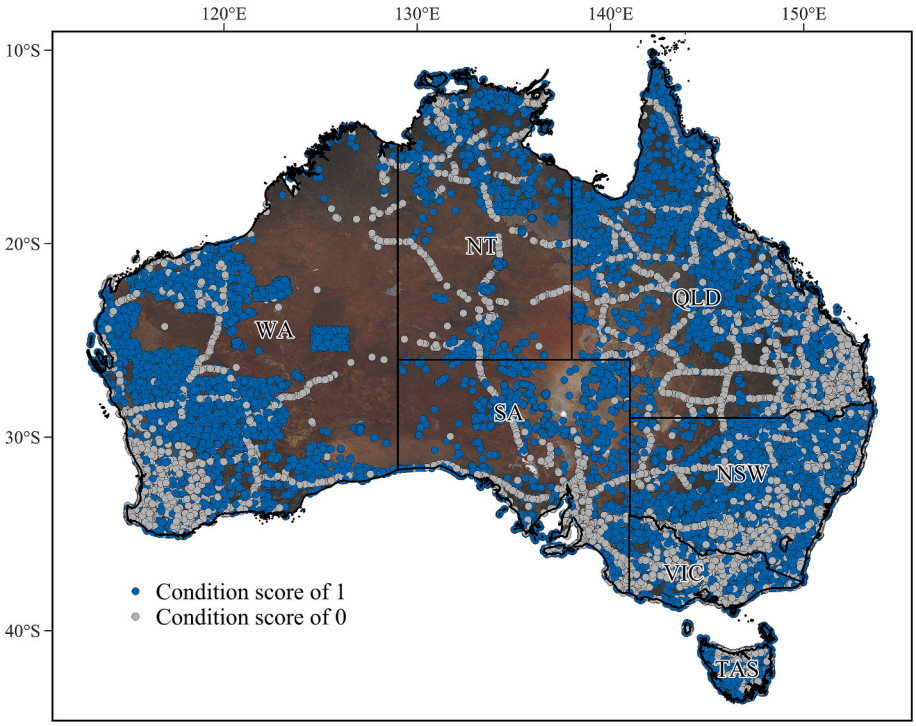

Fig. 1. Distribution of ground-based ecosystem condition scores across Australia (showing states and territories) used as input data in the deep learning model. Blue indicators have a condition score of 1 (at or near reference condition), grey indicators have a condition score of 0 (degraded).

month, and mean minimum temperature of the coldest month (Harwood et al., 2018).

2.3. Deep learning workflow

For each ground data point to be input into the deep learning model, all Landsat observations were extracted for the calendar year of the ground data survey (e.g. for a survey completed on 14 May 2009, all observations were extracted for 2009). Spectral indices were then generated for each observation. Landsat observations of each variable (i.e. spectral reflectance, spectral indices) were grouped as bimonthly and monthly data due to a) variability in number of reoccurring Landsat observations across the continent, and b) model architecture for the kernel to operate over time series data of the same length. For bimonthly and monthly data, the minimum, maximum and median of the grouped observations were calculated. For bimonthly and monthly data, 6 or 12 observations respectively may not have been generated for a ground data point, due to issues of cloud cover or no observation. In this case, where one observation was missing with valid observations before and after, the missing data were linearly interpolated, however where consecutive observations were not record, this data were not used as input data to the model. For each ground data point, contextual data were extracted from relevant topographical and climatological datasets, as well as latitude, longitude and survey year. Finally, input data were normalised for each variable based on global 2nd and 98th percentile normalisation as recommended for models with similar architecture (Pelletier et al., 2019; Zhu et al., 2021).

Our deep learning model architecture was inspired by the temporal convolutional neural network proposed by Pelletier et al. (2019), and our deep learning workflow considered input from other applications using similar model architecture (Miller et al., 2023; Wang et al., 2021; Zhu et al., 2021) (Fig. 2). Our model included three temporal convolutional layers (64 units) used for time series data (Fig. 2). To avoid model overfitting this architecture implemented regulation mechanisms including dropout and batch normalisation after each convolutional layer (Pelletier et al., 2019; Zhu et al., 2021). The convolutional layers of the time series data were concatenated with the context data as a flattened layer into a fully connected neural network (dense) layer (256 units). A final dense layer was used to produce outputs of the probability of ecosystem condition being at our near reference condition (1) as opposed to being degraded (0).

The model was generated using the Adam optimiser with default parameters (Kingma and Ba, 2017), implemented with the Keras library (Chollet et al., 2015) using the Tensorflow backend (Abadi et al., 2016). Model architecture design from Keras is provided in Fig. S1. Several model iterations were generated with varying input data. This included using monthly or bimonthly data, using minimum, maximum or median aggregates of time series observations, and varying combinations of contextual data. Over 50 models were generated using the same model architecture. The final model selection was based on lowest validation loss, highest validation accuracy and the lowest number of input data layers (see Section 2.4).

The selected final model was applied to make predictions across the Australian continent for the calendar years 2010, 2015, 2020, 2021, 2022. EO time series data were generated using the same approach as input data for model training, including normalisation of data variables and interpolation of values where required in time series observations. The model was applied to Landsat data resampled to 100 m spatial resolution. This resampling from 30 m (approximate native Landsat resolution) to 100 m was deemed appropriate due to computational requirements of generating a continental scale ecosystem condition map to demonstrate this approach. Model application was parallelised using Dask (Rocklin, 2015), whereby this model can be applied at 30 m resolution based on future user requirements.

2.4. Model evaluation and validation

To evaluate the performance of our models, input data ($n = 209,041$) were randomly split into training (60%; $n = 125,424$), testing (20%; $n = 41,808$) and validation (20%; n = 41,809) datasets, where no input data were of both the same location and time period. Training data were used to perform the initial training of the model, initialising the weights of the neural network. Validation data were used for tuning the neural networks hyperparameters and comparing how these changes affect the predictive capacity of the model. Testing data were used to evaluate the predictive accuracy of the neural network on data that had not been used to train or validate the model. Model assessment was based on the convergence of training and validation accuracy and training and validation loss parameters. Considerations were also made for selecting a suitable model based on model complexity, including training time and number of covariate input data. Distribution of ecosystem condition values from model predictions based on input data were also analysed to evaluate model output. To identify variable importance of input time series covariate data, shapely additive explanations (SHAP) analysis was

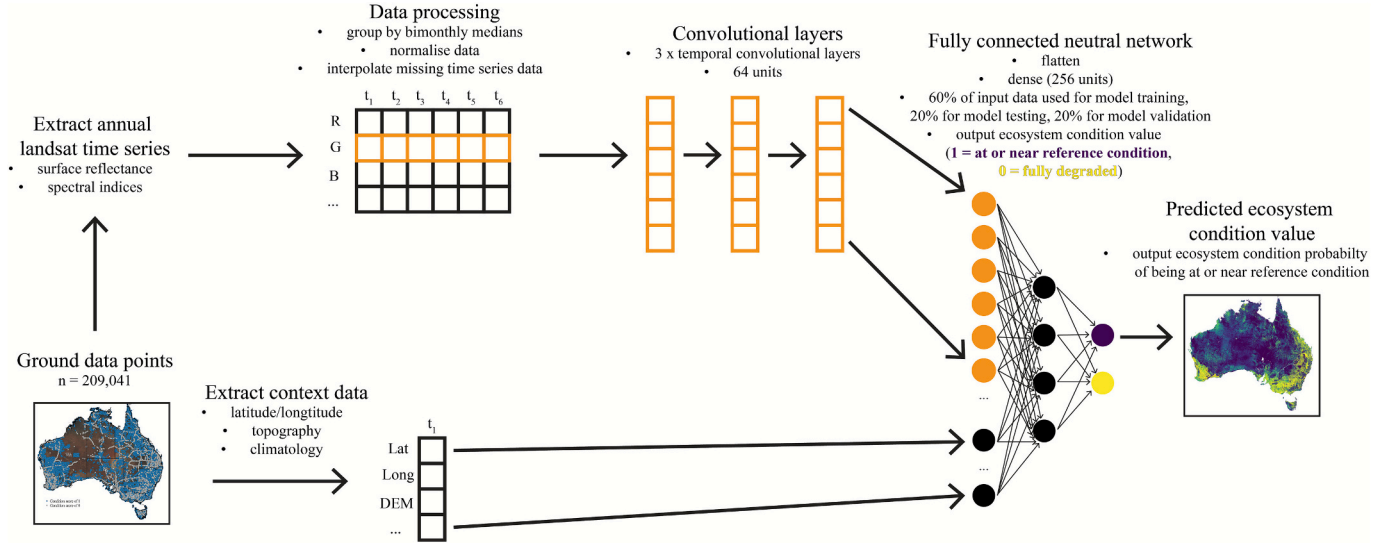

Fig. 2. Deep learning workflow used in this study to model ecosystem condition for a specified year. Note the convolutional layers are the shape of 6 time series (t) stacked on each other for all 23 variables (6 x 23 = 138 variables total). For full model architecture see Figure S1.

undertaken, which provides insight into variable importance of complex machine learning models (Lundberg and Lee, 2017).

2.5. Model sensitivity

Spatial and temporal sensitivity of the model was evaluated across the Australian continent for the five calendar year maps. Spatial variation was mapped, stratified on bioregions, where mean absolute error (MAE) of predicted and actual ecosystem condition values were summarised. Temporal variation was mapped to evaluate predicted ecosystem condition values over time. This was achieved by mapping the standard deviation of each pixel for all years mapped. Predicted ecosystem condition values were summarised for each year to provide a continental and state and territory summary of mean ecosystem condition. Similarly, distribution of predicted values from model outputs for each year were summarised. Furthermore, predicted ecosystem condition in this study was compared with the Habitat Condition Assessment System (HCAS; (Valavi et al., 2025)) across Australia for years 2010, 2015, 2020, 2021 and 2022. This included a difference image for each year as well as kernel density estimates to compare the distribution of ecosystem condition values for the two datasets (Figs. S3 and S4).

3. Results

3.1. Model evaluation and validation

The final model provided accurate predictions for national scale mapping of ecosystem condition. This model was based on bimonthly median time series inputs from EO data. The model consisted of the 6 spectral bands, 17 spectral indices, and 8 topographical and climatological layers (latitude, longitude, elevation, topographic wetness index, mean annual potential evaporation, mean annual precipitation, mean minimum temperature of the coldest month, mean maximum temperature of the warmest month). The model had a batch size of 32 and was run for 500 epochs. This resulted in a loss function of 0.1839, an accuracy of 0.9368, with a validation loss of 0.1336, and validation accuracy of 0.9553. These evaluation metrics suggest the model performs satisfactorily with relatively low loss and high accuracy on both training and validation sets. The similar performance of the validation set compared to the training set suggests the model generalises well on data that had not been used to train or validate the model.

SHAP analysis demonstrated the importance of topological and climatological contextual data when describing variance for ecosystem condition across the Australian continent (Fig. S2). In particular, mean maximum temperature of the warmest month and mean minimum temperature of the coldest month were the most important variables in the model. Latitude and longitude were also highly contributing factors, demonstrating the spatial variation of ecosystem condition across the continent. The derived spectral index of normalised burn ratio (NBR) was the most important variable in describing ecosystem condition using Earth observation time series. Other highly contributing time series inputs including the normalised difference water index (NDWI), normalised difference vegetation index (NDVI), bare soil index (BSI) and the green spectral band. These indices demonstrate vegetation phenology and moisture are important factors for evaluating ecosystem condition.

The distribution of ecosystem condition values from model predictions based on input data suggest the model generalises well over space and time (Fig. 3). Observed values of ecosystem condition for input data considered degraded (0) show a distribution where predicted values are also 0 (median = 0, 25% quartile = 0, 75% quartile = 0.1). Observed values for input data of ecosystem condition values considered in reference condition (1) also demonstrate the model capacity to predict values of reference condition. However, the distribution of predicted values shows areas considered high condition but lower than reference (e.g. greater than 0.8 proportion native species) more difficult to differentiate from areas of reference condition (1) (median = 0.9, 25% quartile = 0.6, 75% quartile = 1) (Fig. 3).

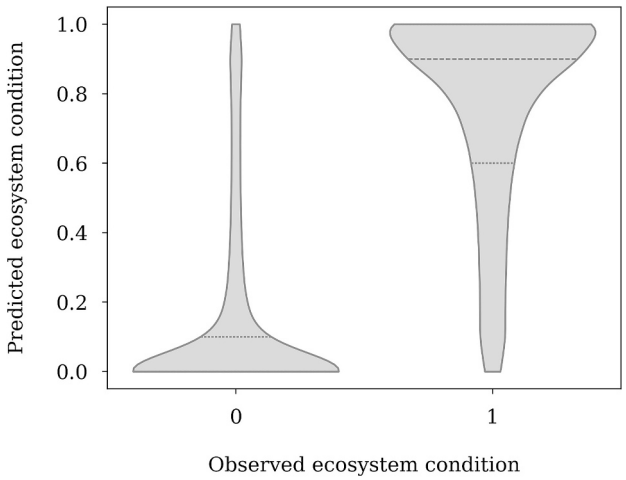

Fig. 3. Distribution of ecosystem condition values from model predictions based on input (train/test/validation) data, where 0 indicates a fully degraded condition and 1 indicates at or near reference condition. Volin plot statistics include the interquartile range (IQR; denoted by the solid grey lines at both 0.0 and 1.0 (y-axis) for each observed ecosystem condition state (x axis)) as well as quartile lines (dotted grey lines; where not visible indicates quartile is at predicted ecosystem condition of either 0.0 or 1.0 (y-axis)).

3.2. Model outputs

Annual continental-scale ecosystem condition maps were produced for Australia for the calendar years 2010, 2015, 2020, 2021 and 2022 at 100 m spatial resolution (Fig. 4). Predicted ecosystem condition maps are available and accessible on the CSIRO data access portal (https://data.csiro.au/collection/csiro:65931). Mean predicted ecosystem condition across Australia was greater than 0.65 for all years (Fig. 6a), however with considerable spatial variability. Arid regions in Australia's interior had predicted condition scores close to 1 for all years. Highly modified landscapes on Australia's southeastern and southwestern regions had predicted condition scores closer to 0 for all years. Predictions of ecosystem condition for 2020 differ somewhat compared to other years, particularly in the north of the continent and southeast of the continent, with lower ecosystem condition scores, potentially associated with severe bushfire activity (Godfree et al., 2021).

3.3. Model sensitivity and landscape variability

Spatial and temporal variability of predicted ecosystem condition across the Australian continent demonstrates a) the model's sensitivity and capacity to generalise well, and b) landscape variability across the Australian continent (Fig. 5). The spatial variability of the mean absolute error (MAE) of predicted and observed ecosystem condition values across Australia's bioregions (DCCEEW, 2020) demonstrates how diverse the Australian landscape can be. Overall, 96% of bioregions had an MAE value of less than 0.4, with over 40% of bioregions having MAE values less than 0.2, indicating strong agreement between predicted and observed ecosystem condition values. Areas of low MAE values were associated with highly modified landscapes of southeastern and southwestern Australia. These highly modified landscapes, though often mosaicked in land cover and land use, demonstrate relative stability as low condition areas that the model can accurately identify (Fig. 5a). Regions where MAE values were slightly higher (i.e. greater than 0.3 and below 0.5 MAE) are associated with landscapes that can experienced high natural variability associated with rainfall, evapotranspiration, and vegetation cover, that may have considerable influence on

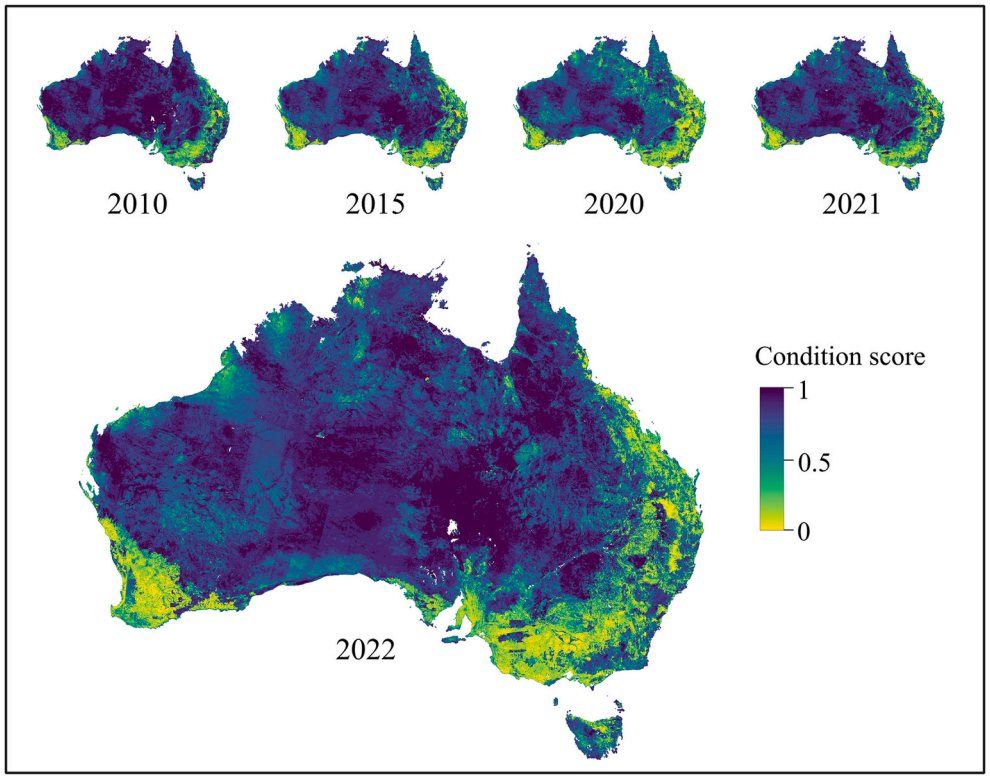

Fig. 4. Predicted ecosystem condition across Australia for years 2010, 2015, 2020, 2021 and 2022. Condition score of 1 indicates at or near reference condition (i.e. 100 % proportion of native species as a surrogate measure of ecosystem condition). Condition score of 0 indicates a fully degraded condition (i.e. 0 % proportion of native species as a surrogate measure of ecosystem condition).

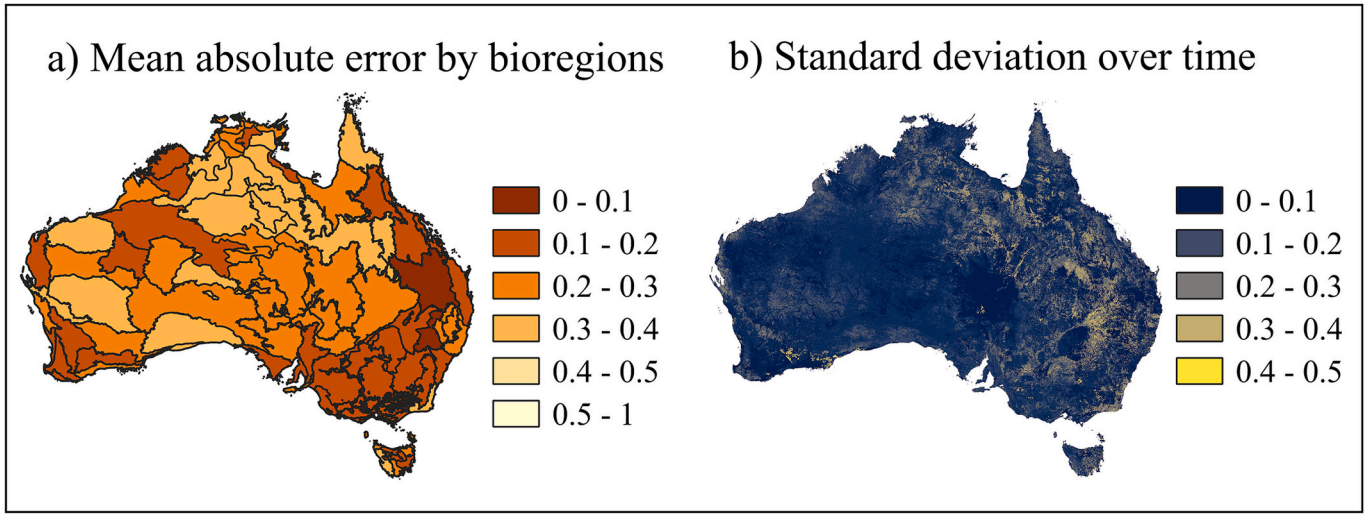

Fig. 5. Spatial and temporal model sensitivity and landscape variability. a) Mean absolute error (MAE) of predicted ecosystem condition values summarised by Australia's bioregions (IBRA version 7; (DCCEEW, 2020)). b) Standard deviation of each pixels predicted ecosystem condition value over time, for all years mapped (2010, 2015, 2020, 2021, 2022).

vegetation phenology and landscape characteristics observed using EO data (e.g. savannahs of northern Australia where vegetation response is driven by wet and dry season dynamics (Guerschman et al., 2009) and around waterholes were lateral inflows drive vegetation response (Henriques et al., 2024)).

Arid landscapes in the interior, as well as highly modified and populous landscapes in the southeast and southwest, demonstrate relative temporal stability, with standard deviation values less than 0.3 (Fig. 5b). In comparison, areas with higher temporal variability are associated with rangeland areas of mixed native vegetation and predominately pastoral land use in the east and northeast of the continent. These landscapes had standard deviation values ranging from 0.2 to 0.5. Given the model generalises well spatially and temporally elsewhere on the continent, the temporal variability associated with rangeland landscapes may be associated with rainfall variability and changing grazing pressures, where ecosystem condition may fluctuate within years and be difficult to estimate due to model insensitivity (as observed in other continental ecosystem condition products, see Fig. S3 and S4).

The time series of predicted ecosystem condition across Australia demonstrated broad scale consistency and stability (Fig. 6). The Northern Territory (NT) and South Australia (SA) consistently demonstrated mean predicted ecosystem condition values across the mapped calendar years higher than other states and territories. This is likely due to relatively lower human impact than other states and territories across Australia, as well as substantial areas of arid regions. Together with Western Australia (WA), all were consistently above the national mean (Fig. 6a). New South Wales (NSW), the Australian Capital Territory (ACT) and Victoria (VIC) exhibited lower mean predicted condition values than other states and territories.

The majority of Australia had predicted ecosystem condition values greater than 0.5 (Fig. 6b). All years, with the exception of 2020, exhibit similar distributions of predicted values of ecosystem condition (Fig. 6b). A broader and lower range of condition values was predicted for 2020 (mean = 0.64, median = 0.7, 25% quartile = 0.4, 75% quartile = 0.9). Greatest reductions in mean condition values for 2020 were predicted in with NSW, NT and SA.

4. Discussion

This study demonstrates how an innovative deep learning approach can overcome the challenges of remotely estimating ecosystem condition dynamically across a large and diverse continent. In this study we assumed a direct relationship between ecosystem condition and the proportion of native species observed in vegetation surveys. Earth observation data were used with a deep learning workflow demonstrating the capacity to predict ecosystem condition across Australia at 100 m resolution. This approach pairs time series information with known on ground condition data that accounts for vegetation phenology, with a model that generalises well over space and time. Evaluation of this approach for identifying changes in ecosystem condition within the context of natural variation of ecosystems was demonstrated by generating several annual maps (2010, 2015, 2020, 2021, 2022) with a model validation accuracy of 0.9553. Mean predicted ecosystem condition was greater than 0.65 for all years, however with considerable spatial variability. Arid regions in Australia's interior demonstrated predicted condition scores close to 1 for all years, compared to regions in Australia of highly modified landscapes in the southeastern and southwestern parts of the continent. Predicted values across the continent demonstrated temporal stability in arid and highly modified regions of the continent, however, areas with high rainfall variability and seasonal variability in land use (e.g. grazing pressures) often had greater temporal variation in predicted ecosystem condition. The results of this study demonstrate that using deep learning techniques and Earth observation data time series can provide quantitative information on ecosystem condition, where temporal variability of vegetation phenology and spatial variability of bioregions can be accounted for.

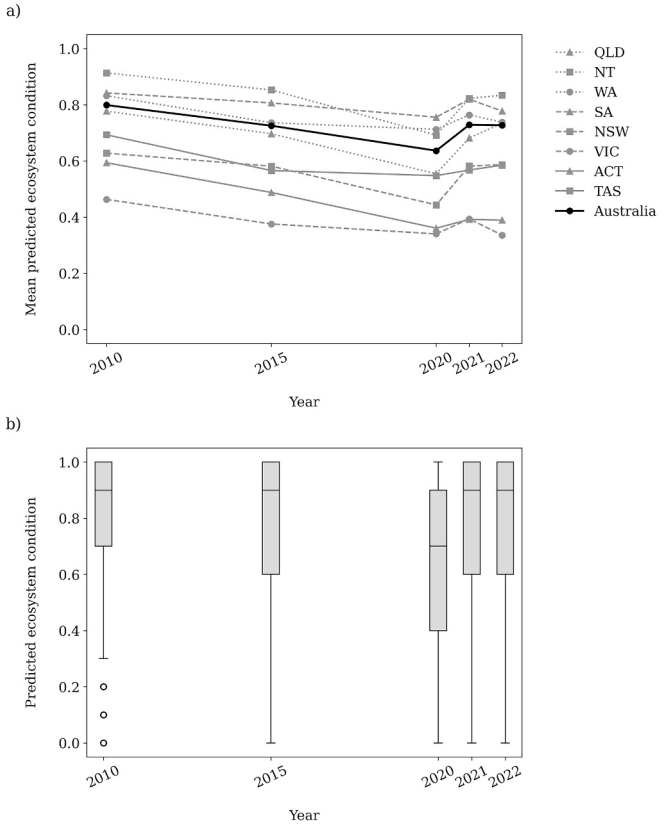

Fig. 6. Time series of a) mean predicted condition for each Australian State and Territory as per model outputs and b) distribution of predicted condition values of all of Australia for each year. Box plot statistics include the median (internal horizontal line), interquartile range (IQR; denoted by the box), and whiskers are calculated as ± 1.58 x IQR $\sqrt{n}$.

4.1. Ecosystem condition of Australia

Broad spatial and temporal patterns in predicted ecosystem condition are generally consistent with previous continental modelled approaches (Donohue et al., 2013; Harwood et al., 2016; Valavi et al., 2025). Highly modified landscapes typically had very low predicted ecosystem condition values (near 0), including areas of southeastern and southwestern Australia which are more populous with higher agricultural intensity. For the time series presented in this study, highly modified landscapes demonstrate relatively consistent ecosystem condition values close to 0, where a trajectory of greater degradation of ecosystems can be observed in areas that fringe highly modified regions, where agriculture expansion has occurred in recent decades (McFarlane and Wallace, 2019; Newell et al., 2006; OEH and CSIRO, 2019; White et al., 2020). Areas of high predicted ecosystem condition (near 1) were identified in Australia's remote regions, such as Australia's interior, Gulf of Carpentaria, Arnhem land, and Exmouth Gulf (Fig. 4). Relatively high predicted ecosystem condition was also prevalent in protected areas such as national parks. The temporal stability of these relatively intact areas varied across the continent. High condition areas in WA had large variability in predicted condition scores over time which may be associated with vegetation response to climatological factors (Fig. 5a).

Our results echo previous research that identifies some areas across Australia with high temporal variability in ecosystem condition (Donohue et al., 2013; Lawley et al., 2016; Newell et al., 2006). This is particularly evident in our results with temporal changes that occur across the central QLD rangelands and into the NT towards Arnhem land (Figs. 4, 5b). The variation in the time series suggests that our mapping of ecosystem condition could be associated with a combination of changing rainfall patterns and variable land use patterns (e.g. rangeland grazing dynamics such as stocking and destocking pastures) which can be challenging to identify from remote sensing (Bastin et al., 2012). However, from an ecological perspective, within and between year ecosystem dynamics associated with natural or simulated natural disturbance regimes are generally not considered to indicate condition change, when these occur within an intact, inter-connected landscape (Richards et al., 2020). The complex and varying response of Australia's vegetation to landscape change in different bioregions makes evaluation of broad scale factors to changes in ecosystem condition challenging, particularly those that may be more evident at regional scales (Legge et al., 2023). In addition, oscillations in condition scores across the time series in both relatively intact and relatively degraded regions may demonstrate areas of low confidence in the model that coincide with limited input ground data for model training (e.g. central WA and central west rangelands of Tasmania). Nevertheless, our results also

demonstrate broad stability of Australia's ecosystem condition at a continental scale, with a mean ecosystem condition across Australia for all mapped years of 0.65.

4.2. Earth observation time series with deep learning techniques

This study demonstrates the utility of deep learning techniques for environmental applications. More recently, additional environmental spatial covariates have been incorporated with the deep learning workflows to complement contextual time series data with static long-term contextual environmental data (Rao et al., 2020; Zhu et al., 2021). This addition is also adopted in the workflow presented in this study, where Landsat time series data were coupled with spatial data on topographic and climatological factors, providing spatial and temporal context to predicting ecosystem condition. Conceptually this is an ideal approach as ecosystem condition can be considered as a context-driven quantification problem (Henrys and Jarvis, 2019; McNellie et al., 2020; Yen et al., 2019).

Estimating ecosystem condition from Earth observation data requires contextualisation. Spectral signatures of vegetation from different landscapes may be similar, yet diverge considerably in observed habitat condition (Harwood et al., 2016). For example, an open eucalypt woodland in a temperate location that may be considered relatively pristine, may exhibit a similar spectral signature measured through EO data as a tropical closed canopy forest in a degraded state (Williams et al., 2024). Providing contextual information on these spectral signatures, through time series deep learning approaches coupled with data on topographic and climatological factors, may provide greater capacity for accurate prediction of ecosystem condition (Ma et al., 2024). In addition, generating meaningful metrics of ecosystem condition, relating to structure, function and composition, is challenging due to the complex relationships between these indicators and observed ecosystem condition (McNellie et al., 2020; Nicholson et al., 2021). Using Earth observations to derive these metrics as a snapshot or mean dataset of generalised condition may not provide sufficient information to accurately determine changes in ecosystem condition. For example, vegetation phenological characteristics can vary within a calendar year and it may be important to consider this variation in the spectral signature to understand natural variability and determine ecosystem condition in varying states of intact or degraded condition (McFarlane and Wallace, 2019; Nagendra et al., 2013; Pettorelli et al., 2018; Schneider et al., 2017; Yang et al., 2025). The capacity of time series CNN models align with a conceptual context-driven approach to identifying ecosystem condition (McNellie et al., 2020; Tehrany et al., 2017). This contrasts with previous Earth observation approaches that initially provided limited insight into ecosystem condition change over time (Harwood et al., 2016), although subsequent versions of HCAS (e.g. Valavi et al., 2025) demonstrate capacity to provide annual time series with broadly similar patterns at continental scale to this study (Fig. S3 and S4). Moreover, the deep learning model architecture demonstrates capability of temporal as well as spatial contextual predictions for a pixel (Miller et al., 2024), without the need to benchmark relative changes in ecosystem condition to a reference state in close environmental proximity (e.g. (Harwood et al., 2016)).

4.3. Considerations of deep learning models for ecosystem condition mapping

The approach demonstrated in this study does provide some considerations for further continental scale maps of ecosystem condition. For this study, input data to this model was labelled only as either at or near reference condition (1) or fully degraded condition (0). Interpretation of the map outputs presents the probability associated with a pixel being at or near reference condition (i.e. 100% native species as a surrogate measure of ecosystem condition). We demonstrate that the model generalised well, with limited overfitting identified, and overall good performance. For quantifying ecosystem condition using deep learning, we suggest this is best represented and communicated as a continuous attribute, as categorical approaches (e.g. pristine, fair, poor condition) can be difficult to interpret.

The use of EO data also presents challenges that are inherently difficult to resolve (Pasetto et al., 2018; Pettorelli et al., 2018). In our approach we observed issues with scan line error of Landsat 7; however, observations were utilised where required to ensure each pixel had a bimonthly observation to enable consistent prediction of ecosystem condition across the continent. In some cases, we observed considerable variation between some years and regions of ecosystem condition predictions, and these may be due to minor variations in spectral reflectance associated with using all available Landsat satellite sensors for selected years (i.e. Landsat 5, 7, 8) (Lewis et al., 2017; Roy et al., 2016). Our approach reduced annual Landsat observations to bimonthly means (i.e. 6 time series observations per calendar year). This may seem reductive of the available time series data for Australia; however, substantial variation in spectral signatures of time series data may be challenging for the model to anticipate variation within particular landscapes. Optimising time series information from EO data (e.g. landscape variation vs noise) for model predictions over large spatial extents requires further research.

4.4. Opportunities for continental ecosystem condition mapping

Several opportunities exist for ecosystem condition mapping at continental and global extents using EO data and deep learning techniques (Miller et al., 2024; Skidmore et al., 2021). Importantly, conceptual definitions of ecosystem condition must be ecologically meaningful and mappable across space and time (McNellie et al., 2020; Nicholson et al., 2021; Skidmore et al., 2021). Our approach maps the proportion of native species present in the landscape as a surrogate measure of ecosystem condition. Further, we suggest that across Australia, the proportion of native to non-native species have different spectral signatures associated with Earth observation time series. Our approach assumes that native species have relatively consistent spectral signatures throughout the calendar year due to being predominantly evergreen, or that native species in areas of distinct seasonality follow this trend, such as in the tropical wet and dry seasons and much of arid/semi-arid central Australia (Donohue et al., 2009). We also assume that non-native species have highly variable spectral signatures or signatures with particular regular trends (e.g. crops), as well as potentially stable signatures (e.g. *Pinus radiata* plantations), but dissimilar to vegetation phenological signatures, such as artificial surfaces and water bodies. These assumptions may be refined for future approaches using EO data, and conceptual definitions might therefore need to be modified to suit varying temporal and spatial scales to ensure output maps are fit for purpose. Nevertheless, awareness of using EO measures as indicators for ecosystem condition, and the need to consider biophysical relationships of the sensor-to-landscape characteristics, are required for meaningful measures of quantifying ecosystem condition.

We utilised the Landsat imagery archive resampled to 100 m resolution to pair time series information with known on-ground condition that accounts for vegetation phenology. Further work should pursue using input data for a range of ecosystem condition values between 0 and 1 to provide greater confidence where ecosystem condition may be in a partially modified state. In addition, incorporating dynamic climatological context layers (e.g. annual rainfall anomaly) would align to time series inputs that may result in a higher degree of landscape variability to help inform the model. This may also provide greater evaluation of model sensitivity and natural landscape variability over space and time. In particular, approaches that provide greater confidence for ecosystem condition predictions that identify gradual changes in ecosystems over time, and are able generalise over large spatial and temporal context, will provide greater capacity to utilise continental scale maps for informing potential management intervention. This may

be complemented by EO time series of greater spectral and temporal resolution (e.g. Sentinel-2, Planet scope).

5. Conclusion

This study presents a new approach to map continental ecosystem condition using time series satellite imagery and innovative deep learning techniques. We demonstrate that this approach can overcome the challenges of estimating ecosystem condition remotely, associated with phenological variation. Our model generalised well over space and time to predict ecosystem condition scores by assuming a direction relationship to the proportion of native species present in the landscape. Utilising innovative deep learning approaches, such as those that account for spectral variation in time series and facilitate the integration of topological and climatological datasets, provide context-driven approaches that align with a conceptual framework of ecosystem condition.

CRediT authorship contribution statement

Christopher J. Owers: Writing – review & editing, Writing – original draft, Software, Methodology, Formal analysis, Data curation. **Karel Mokany:** Writing – review & editing, Supervision, Methodology, Funding acquisition, Conceptualization. **Chris Ware:** Writing – review & editing, Software, Data curation. **Thomas D. Harwood:** Writing – review & editing, Supervision, Conceptualization. **Jinyan Yang:** Writing – review & editing, Data curation. **Randall J. Donohue:** Writing – review & editing, Supervision. **Tim R. McVicar:** Writing – review & editing, Supervision. **Eric A. Lehmann:** Writing – review & editing, Software. **Kristen J. Willams:** Writing – review & editing, Supervision, Data curation, Conceptualization. **Rebecca K. Schmidt:** Supervision, Conceptualization. **Matt Paget:** Supervision, Software, Methodology. **Simon Ferrier:** Writing – review & editing, Supervision, Conceptualization. **Charlotte Pelletier:** Writing – review & editing, Software.

Declaration of competing interest

The authors declare that they have no known competing financial interests or personal relationships that could have appeared to influence the work reported in this paper.

Acknowledgements

This research was an outcome of a CERC Postdoctoral Fellowship at CSIRO awarded to CJO. Compute and support for analysis was provided through the CSIRO EASI platform as well as CSIRO HPC facilities.

Appendix A. Supplementary data

Supplementary data to this article can be found online at https://doi.org/10.1016/j.ecoinf.2026.103639.

Data availability

Predicted ecosystem condition maps: https://data.csiro.au/collection/csiro:65931

References

AARSC, 2021. Australian Tree Crops. https://www.une.edu.au/research/research-centres-institutes/applied-agricultural-remote-sensing-centre/collaborative-r-and-d-opportunities/industry-applications-and-maps/australian-tree-crops.

Abadi, M., Barham, P., Chen, J., Chen, Z., Davis, A., Dean, J., Devin, M., Ghemawat, S., Irving, G., Isard, M., Kudlur, M., Levenberg, J., Monga, R., Moore, S., Murray, D.G., Steiner, B., Tucker, P., Vasudevan, V., Warden, P., Wicke, M., Yu, Y., Zheng, X., 2016. TensorFlow: A System for Large-scale Machine Learning. https://doi.org/10.48550/arXiv.1605.08695.

ABARES, 2021. Australia's Plantations 2020–21. https://www.agriculture.gov.au/abares/forestsaustralia/forest-data-maps-and-tools/spatial-data/australias-plantations.

Bastin, G., Scarth, P., Chewings, V., Sparrow, A., Denham, R., Schmidt, M., O'Reagain, P., Shepherd, R., Abbott, B., 2012. Separating grazing and rainfall effects at regional scale using remote sensing imagery: a dynamic reference-cover method. Remote Sens. Environ. 121, 443–457. https://doi.org/10.1016/j.rse.2012.02.021.

Beck, H.E., Zimmermann, N.E., McVicar, T.R., Vergopolan, N., Berg, A., Wood, E.F., 2018. Present and future köppen-Geiger climate classification maps at 1-km resolution. Sci. Data 5, 1–12. https://doi.org/10.1038/sdata.2018.214.

Beck, H.E., McVicar, T.R., Vergopolan, N., Berg, A., Lutsko, N.J., Dufour, A., Zeng, Z., Jiang, X., van Dijk, A.I.J.M., Miralles, D.G., 2023. High-resolution (1 km) Köppen-Geiger maps for 1901–2099 based on constrained CMIP6 projections. Sci. Data 10, 724. https://doi.org/10.1038/s41597-023-02549-6.

BOM, 2012. Record Breaking La Nina Events. Australia Government Bureau of Meteorology, Melbourne, Australia. https://www.bom.gov.au/climate/enso/history/.

BOM, 2016. Annual Climate Report 2015. Australia Government Bureau of Meteorology, Melbourne, Australia. https://www.bom.gov.au/climate/annual_sum/2015/.

Byrne, G., Broomhall, M., Walsh, A.J., Thankappan, M., Hay, E., Li, F., McAtee, B., Garcia, R., Anstee, J., Kerrisk, G., Drayson, N., Barnetson, J., Samford, I., Denham, R., 2024. Validating Digital Earth Australia NBART for the Landsat 9 Underfly of Landsat 8. Remote Sens. 16, 1233. https://doi.org/10.3390/rs16071233.

Ceballos, G., Ehrlich, P.R., Barnosky, A.D., García, A., Pringle, R.M., Palmer, T.M., 2015. Accelerated modern human–induced species losses: entering the sixth mass extinction. Sci. Adv. 1, e1400253. https://doi.org/10.1126/sciadv.1400253.

Chase, J.M., Blowes, S.A., Knight, T.M., Gerstner, K., May, F., 2020. Ecosystem decay exacerbates biodiversity loss with habitat loss. Nature 584, 238–243. https://doi.org/10.1038/s41586-020-2531-2.

Chauhan, R., Ghanshala, K.K., Joshi, R.C., 2018. Convolutional neural network (CNN) for image detection and recognition. In: 2018 First International Conference on Secure Cyber Computing and communication (ICSCCC). Presented at the 2018 First International Conference on Secure Cyber Computing and Communication (ICSCCC), pp. 278–282. https://doi.org/10.1109/ICSCCC.2018.8703316.

Chollet, F., et al., 2015. Keras. https://keras.io.

Cresswell, I., Janke, T., Johnston, 2021. Australia State of the Environment 2021: Overview. Australian Government Minister for the Environment, Commonwealth of Australia, Canberra, Australia. https://doi.org/10.26194/f1rh-7r05.

DCCEEW, 2020. Interim Biogeographic Regionalisation for Australia v. 7 (IBRA). Department of Climate Change, Energy, the Environment and Water. https://www.dcceew.gov.au/environment/land/nrs/science/ibra.

Dhu, T., Dunn, B., Lewis, B., Lymburner, L., Mueller, N., Telfer, E., Lewis, A., McIntyre, A., Minchin, S., Phillips, C., 2017. Digital earth Australia – unlocking new value from earth observation data. Big Earth Data 1, 64–74. https://doi.org/10.1080/20964471.2017.1402490.

Díaz, S., Malhi, Y., 2022. Biodiversity: concepts, patterns, trends, and perspectives. Annu. Rev. Env. Resour. 47, 31–63. https://doi.org/10.1146/annurev-environ-120120-054300.

Donohue, R.J., McVicar, T.R., Roderick, M.L., 2009. Climate-related trends in Australian vegetation cover as inferred from satellite observations, 1981-2006. Glob. Chang. Biol. 15, 1025–1039. https://doi.org/10.1111/j.1365-2486.2008.01746.x.

Donohue, R.J., Harwood, T.D., Williams, K.J., Ferrier, S., McVicar, T.R., 2013. Estimating habitat condition using time series remote sensing and ecological survey data. In: CSIRO Earth Observation and Informatics Transformational Capability Platform Client Report EP1311716 44. https://publications.csiro.au/rpr/pub?pid=csiro:EP1311716.

Farr, T.G., Rosen, P.A., Caro, E., Crippen, R., Duren, R., Hensley, S., Kobrick, M., Paller, M., Rodriguez, E., Roth, L., Seal, D., Shaffer, S., Shimada, J., Umland, J., Werner, M., Oskin, M., Burbank, D., Alsdorf, D., 2007. The shuttle radar topography mission. Rev. Geophys. 45. https://doi.org/10.1029/2005RG000183.

Gallant, J.C., Austin, J.M., 2015. Derivation of terrain covariates for digital soil mapping in Australia. Soil Res. 53, 895–906. https://doi.org/10.1071/SR14271.

Godfree, R.C., Knerr, N., Encinas-Viso, F., Albrecht, D., Bush, D., Christine Cargill, D., Clements, M., Gueidan, C., Guja, L.K., Harwood, T., Joseph, L., Lepschi, B., Nargar, K., Schmidt-Lebuhn, A., Broadhurst, L.M., 2021. Implications of the 2019–2020 megafires for the biogeography and conservation of Australian vegetation. Nat. Commun. 12, 1023. https://doi.org/10.1038/s41467-021-21266-5.

Gomes, E., Inácio, M., Bogdzevič, K., Kalinauskas, M., Karnauskaitė, D., Pereira, P., 2021. Future land-use changes and its impacts on terrestrial ecosystem services: a review. Sci. Total Environ. 781, 146716. https://doi.org/10.1016/j.scitotenv.2021.146716.

Guerschman, J.P., Hill, M.J., Renzullo, L.J., Barrett, D.J., Marks, A.S., Botha, E.J., 2009. Estimating fractional cover of photosynthetic vegetation, non-photosynthetic vegetation and bare soil in the Australian tropical savanna region upscaling the EO-1 Hyperion and MODIS sensors. Remote Sens. Environ. 113, 928–945. https://doi.org/10.1016/j.rse.2009.01.006.

Hansen, A.J., Noble, B.P., Veneros, J., East, A., Goetz, S.J., Supples, C., Watson, J.E.M., Jantz, P.A., Pillay, R., Jetz, W., Ferrier, S., Grantham, H.S., Evans, T.D., Ervin, J., Venter, O., Virnig, A.L.S., 2021. Toward monitoring forest ecosystem integrity within the post-2020 Global Biodiversity Framework. Conserv. Lett. 14, e12822. https://doi.org/10.1111/conl.12822.

Harwood, T.D., Donohue, R.J., Williams, K.J., Ferrier, S., McVicar, T.R., Newell, G., White, M., 2016. Habitat condition assessment system: a new way to assess the condition of natural habitats for terrestrial biodiversity across whole regions using

remote sensing data. Methods Ecol. Evol. 7, 1050–1059. https://doi.org/10.1111/2041-210X.12579.
Harwood, T., King, D., Nolan, M., Gallant, J., Ware, C., Austin, J., Williams, K., 2018. 3 Arcsecond Climatology for Continental Australia 1976–2005: Summary Variables with Elevation and Radiative Adjustment For Modelling Biodiversity Patterns. v1. https://doi.org/10.25919/gayv-1e32.
Henriques, M., McVicar, T.R., Holland, K.L., Daly, E., 2024. Extracting vegetation phenology in heterogeneous drylands using LiDAR and Landsat temporal decomposition: a latitudinal assessment of waterholes within the Cooper Creek, Australia. J. Geophys. Res. 129, e2023JG007993. https://doi.org/10.1029/2023JG007993.
Henrys, P.A., Jarvis, S.G., 2019. Integration of ground survey and remote sensing derived data: producing robust indicators of habitat extent and condition. Ecol. Evol. 9, 8104–8112. https://doi.org/10.1002/ece3.5376.
Hooper, D.U., Adair, E.C., Cardinale, B.J., Byrnes, J.E.K., Hungate, B.A., Matulich, K.L., Gonzalez, A., Duffy, J.E., Gamfeldt, L., O'Connor, M.I., 2012. A global synthesis reveals biodiversity loss as a major driver of ecosystem change. Nature 486, 105–108. https://doi.org/10.1038/nature11118.
IPBES, 2019. Summary for Policymakers of the Global Assessment Report on Biodiversity and Ecosystem Services of the Intergovernmental Science-Policy Platform on Biodiversity and Ecosystem Services. IPBES sretariat. https://doi.org/10.1111/padr.12283.
Jaureguiberry, P., Titeux, N., Wiemers, M., Bowler, D.E., Coscieme, L., Golden, A.S., Guerra, C.A., Jacob, U., Takahashi, Y., Settele, J., Díaz, S., Molnár, Z., Purvis, A., 2022. The direct drivers of recent global anthropogenic biodiversity loss. Sci. Adv. 8, eabm9982. https://doi.org/10.1126/sciadv.abm9982.
Johnson, C.N., Balmford, A., Brook, B.W., Buettel, J.C., Galetti, M., Guangchun, L., Wilmshurst, J.M., 2017. Biodiversity losses and conservation responses in the Anthropocene. Science 356, 270–275. https://doi.org/10.1126/science.aam9317.
Karan, M., Liddell, M., Prober, S.M., Arndt, S., Beringer, J., Boer, M., Cleverly, J., Eamus, D., Grace, P., Van Gorsel, E., Hero, J.-M., Hutley, L., Macfarlane, C., Metcalfe, D., Meyer, W., Pendall, E., Sebastian, A., Wardlaw, T., 2016. The Australian SuperSite Network: a continental, long-term terrestrial ecosystem observatory. Sci. Total Environ. 568, 1263–1274. https://doi.org/10.1016/j.scitotenv.2016.05.170.
Kingma, D.P., Ba, J., 2017. Adam: A Method for Stochastic Optimization. https://doi.org/10.48550/arXiv.1412.6980.
Kocev, D., Džeroski, S., White, M.D., Newell, G.R., Griffioen, P., 2009. Using single- and multi-target regression trees and ensembles to model a compound index of vegetation condition. Ecol. Model. 220, 1159–1168. https://doi.org/10.1016/j.ecolmodel.2009.01.037.
Krauss, J., Bommarco, R., Guardiola, M., Heikkinen, R.K., Helm, A., Kuussaari, M., Lindborg, R., Öckinger, E., Pärtel, M., Pino, J., Pöyry, J., Raatikainen, K.M., Sang, A., Stefanescu, C., Teder, T., Zobel, M., Steffan-Dewenter, I., 2010. Habitat fragmentation causes immediate and time-delayed biodiversity loss at different trophic levels. Ecol. Lett. 13, 597–605. https://doi.org/10.1111/j.1461-0248.2010.01457.x.
Lamchin, M., Wang, S.W., Lim, C.H., Ochir, A., Pavel, U., Gebru, B.M., Choi, Y., Jeon, S. W., Lee, W.K., 2020. Understanding global spatio-temporal trends and the relationship between vegetation greenness and climate factors by land cover during 1982–2014. Glob. Ecol. Conserv. 24, e01299. https://doi.org/10.1016/j.gecco.2020.e01299.
Lawley, V., Lewis, M., Clarke, K., Ostendorf, B., 2016. Site-based and remote sensing methods for monitoring indicators of vegetation condition: an Australian review. Ecol. Indic. 60, 1273–1283. https://doi.org/10.1016/j.ecolind.2015.03.021.
Legge, S., Rumpff, L., Garnett, S.T., Woinarski, J.C.Z., 2023. Loss of terrestrial biodiversity in Australia: magnitude, causation, and response. Science 381, 622–631. https://doi.org/10.1126/science.adg7870.
Lewis, A., Oliver, S., Lymburner, L., Evans, B., Wyborn, L., Mueller, N., Raevksi, G., Hooke, J., Woodcock, R., Sixsmith, J., Wu, W., Tan, P., Li, F., Killough, B., Minchin, S., Roberts, D., Ayers, D., Bala, B., Dwyer, J., Dekker, A., Dhu, T., Hicks, A., Ip, A., Purss, M., Richards, C., Sagar, S., Trenham, C., Wang, P., Wang, L.W., 2017. The Australian Geoscience Data Cube — foundations and lessons learned. Remote Sens. Environ. 202, 276–292. https://doi.org/10.1016/j.rse.2017.03.015.
Li, F., Jupp, D.L.B., Thankappan, M., Lymburner, L., Mueller, N., Lewis, A., Held, A., 2012. A physics-based atmospheric and BRDF correction for Landsat data over mountainous terrain. Remote Sens. Environ. 124, 756–770. https://doi.org/10.1016/j.rse.2012.06.018.
Loreau, M., Cardinale, B.J., Isbell, F., Newbold, T., O'Connor, M.I., de Mazancourt, C., 2022. Do not downplay biodiversity loss. Nature 601, E27–E28. https://doi.org/10.1038/s41586-021-04179-7.
Love, J., Drielsma, M., Williams, K.J., Thapa, R., 2020. Integrated Model–Data Fusion Approach to Measuring Habitat Condition for Ecological Integrity Reporting: Implementation for Habitat Condition Indicators, Biodiversity Indicator Program Implementation Report. Department of Planning, Industry and Environment NSW, Sydney, Australia. https://nswdpe.intersearch.com.au/nswdpejspui/handle/1/12464.
Lucas, B., Pelletier, C., Schmidt, D., Webb, G.I., Petitjean, F., 2021. A Bayesian-inspired, deep learning-based, semi-supervised domain adaptation technique for land cover mapping. Mach. Learn. 112, 1941–1973. https://doi.org/10.1007/s10994-020-05942-z.
Lundberg, S.M., Lee, S.-I., 2017. A unified approach to interpreting model predictions. In: Advances in Neural Information Processing Systems. Curran Associates, Inc.
Ma, Y., He, T., McVicar, T.R., Liang, S., Liu, T., Peng, W., Song, D.-X., Tian, F., 2024. Quantifying how topography impacts vegetation indices at various spatial and temporal scales. Remote Sens. Environ. 312, 114311. https://doi.org/10.1016/j.rse.2024.114311.
McFarlane, D.J., Wallace, J.F., 2019. Measuring Native Vegetation Extent and Condition Using Remote Sensing Technologies – A Review and Identification of Opportunities. The Western Australian Biodiversity Science Institute, Perth, Australia. https://wabsi.org.au/wp-content/uploads/2019/08/Remote-Sensing-Technologies-Project-Report.pdf.
McNellie, M.J., Oliver, I., Dorrough, J., Ferrier, S., Newell, G., Gibbons, P., 2020. Reference state and benchmark concepts for better biodiversity conservation in contemporary ecosystems. Glob. Chang. Biol. 6702–6714. https://doi.org/10.1111/gcb.15383.
McNellie, M.J., Oliver, I., Ferrier, S., Newell, G., Manion, G., Griffioen, P., White, M., Koen, T., Somerville, M., 2021. Extending vegetation site data and ensemble models to predict patterns of foliage cover and species richness for plant functional groups. Landsc. Ecol. https://doi.org/10.1007/s10980-021-01221-x, 0123456789.
Miller, L., Zhu, L., Yebra, M., Rüdiger, C., Webb, G.I., 2022. Multi-modal temporal CNNs for live fuel moisture content estimation. Environ. Model. Software 156, 105467. https://doi.org/10.1016/j.envsoft.2022.105467.
Miller, L., Zhu, L., Yebra, M., Rüdiger, C., Webb, G.I., 2023. Projecting live fuel moisture content via deep learning. Int. J. Wildland Fire 32, 709–727. https://doi.org/10.1071/WF22188.
Miller, L., Pelletier, C., Webb, G.I., 2024. Deep learning for satellite image time-series analysis: a review. IEEE Geosci. Remote Sens. Magaz. 12, 81–124. https://doi.org/10.1109/MGRS.2024.3393010.
Mokany, K., McCarthy, J.K., Falster, D.S., Gallagher, R.V., Harwood, T.D., Kooyman, R., Westoby, M., 2022. Patterns and drivers of plant diversity across Australia. Ecography 2022, e06426. https://doi.org/10.1111/ecog.06426.
Nagendra, H., Lucas, R., Honrado, J.P., Jongman, R.H.G., Tarantino, C., Adamo, M., Mairota, P., 2013. Remote sensing for conservation monitoring: assessing protected areas, habitat extent, habitat condition, species diversity, and threats. Ecol. Indic. 33, 45–59. https://doi.org/10.1016/j.ecolind.2012.09.014.
National Land and Water Resources Audit, 2001. Australian Native Vegetation Assessment 2001. Commonwealth of Australia, Canberra, Australia. https://www.insidecotton.com/sites/default/files/article-files/pr010286.pdf.
Newell, G.R., White, M.D., Griffioen, P., Conroy, M., 2006. Vegetation condition mapping at a landscape-scale across Victoria. Ecol. Manag. Restor. 7, 2004–2007. https://doi.org/10.1111/j.1442-8903.2006.293_2.x.
Nicholson, E., Watermeyer, K.E., Rowland, J.A., Sato, C.F., Stevenson, S.L., Andrade, A., Brooks, T.M., Burgess, N.D., Cheng, S.-T., Grantham, H.S., Hill, S.L., Keith, D.A., Maron, M., Metzke, D., Murray, N.J., Nelson, C.R., Obura, D., Plumptre, A., Skowno, A.L., Watson, J.E.M., 2021. Scientific foundations for an ecosystem goal, milestones and indicators for the post-2020 global biodiversity framework. Nat. Ecol. Evol. 5, 1338–1349. https://doi.org/10.1038/s41559-021-01538-5.
OEH, CSIRO, 2019. Measuring Biodiversity and Ecological Integrity in NSW Method for the Biodiversity Indicator Program, Office of Environment and Heritage NSW and Commonwealth Scientific and Industrial Research Organisation. NSW Government, Sydney, Australia. https://dev.environment.nsw.gov.au/sites/default/files/measuring-biodiversity-and-ecological-integrity-in-nsw-240127.pdf.
OpenStreetMap contributors, 2017. OpenStreetMap. https://www.openstreetmap.org.
O'Shea, K., Nash, R., 2015. An Introduction to Convolutional Neural Networks. https://doi.org/10.48550/arXiv.1511.08458.
Owers, C.J., Lucas, R.M., Clewley, D., Tissott, B., Chua, S.M.T., Hunt, G., Mueller, N., Planque, C., Punalekar, S.M., Bunting, P., Tan, P., Metternicht, G., 2022. Operational continental-scale land cover mapping of Australia using the Open Data Cube. Int. J. Digit. Earth 15, 1715–1737. https://doi.org/10.1080/17538947.2022.2130461.
Pasetto, D., Arenas-Castro, S., Bustamante, J., Casagrandi, R., Chrysoulakis, N., Cord, A. F., Dittrich, A., Domingo-Marimon, C., El Serafy, G., Karnieli, A., Kordelas, G.A., Manakos, I., Mari, L., Monteiro, A., Palazzi, E., Poursanidis, D., Rinaldo, A., Terzago, S., Ziemba, A., Ziv, G., 2018. Integration of satellite remote sensing data in ecosystem modelling at local scales: practices and trends. Methods Ecol. Evol. 9, 1810–1821. https://doi.org/10.1111/2041-210X.13018.
Pelletier, C., Webb, G.I., Petitjean, F., 2019. Temporal convolutional neural network for the classification of satellite image time series. Remote Sens. 11, 1–25. https://doi.org/10.3390/rs11050523.
Pereira, H.M., Martins, I.S., Rosa, I.M.D., Kim, H., Leadley, P., Popp, A., van Vuuren, D. P., Hurtt, G., Quoss, L., Arneth, A., Baisero, D., Bakkenes, M., Chaplin-Kramer, R., Chini, L., Di Marco, M., Ferrier, S., Fujimori, S., Guerra, C.A., Harfoot, M., Harwood, T.D., Hasegawa, T., Haverd, V., Havlík, P., Hellweg, S., Hilbers, J.P., Hill, S.L.L., Hirata, A., Hoskins, A.J., Humpenöder, F., Janse, J.H., Jetz, W., Johnson, J.A., Krause, A., Leclère, D., Matsui, T., Meijer, J.R., Merow, C., Obersteiner, M., Ohashi, H., De Palma, A., Poulter, B., Purvis, A., Quesada, B., Rondinini, C., Schipper, A.M., Settele, J., Sharp, R., Stehfest, E., Strassburg, B.B.N., Takahashi, K., Talluto, L., Thuiller, W., Titeux, N., Visconti, P., Ware, C., Wolf, F., Alkemade, R., 2024. Global trends and scenarios for terrestrial biodiversity and ecosystem services from 1900 to 2050. Science 384, 458–465. https://doi.org/10.1126/science.adn3441.
Pettorelli, N., Schulte to Bühne, H., Tulloch, A., Dubois, G., Macinnis-Ng, C., Queirós, A. M., Keith, D.A., Wegmann, M., Schrodt, F., Stellmes, M., Sonnenschein, R., Geller, G. N., Roy, S., Somers, B., Murray, N., Bland, L., Geijzendorffer, I., Kerr, J.T., Broszeit, S., Leitão, P.J., Duncan, C., El Serafy, G., He, K.S., Blanchard, J.L., Lucas, R., Mairota, P., Webb, T.J., Nicholson, E., 2018. Satellite remote sensing of ecosystem functions: opportunities, challenges and way forward. Remote Sens. Ecol. Conserv. 4, 71–93. https://doi.org/10.1002/rse2.59.
Rao, K., Williams, A.P., Flefil, J.F., Konings, A.G., 2020. SAR-enhanced mapping of live fuel moisture content. Remote Sens. Environ. 245, 111797. https://doi.org/10.1016/j.rse.2020.111797.

Richards, A.E., Dickson, F., Williams, K.J., Cook, G.D., Murphy, H., Doherty, M., Warnick, A., Metcalfe, D., Prober, S.M., 2020. The Australian Ecosystem Models Framework Project a Conceptual Framework. CSIRO, Australia. http://hdl.handle.net/102.100.100/340404?index=1.

Rocklin, M., Huff, K., Bergstra, J., 2015. Dask: parallel computation with blocked algorithms and task scheduling. In: Proceedings of the 14th Python in Science Conference, pp. 130–136.

Roy, D.P., Kovalskyy, V., Zhang, H.K., Vermote, E.F., Yan, L., Kumar, S.S., Egorov, A., 2016. Characterization of Landsat-7 to Landsat-8 reflective wavelength and normalized difference vegetation index continuity. In: Remote Sensing of Environment, Landsat 8 Science Results, 185, pp. 57–70. https://doi.org/10.1016/j.rse.2015.12.024.

Schneider, F.D., Morsdorf, F., Schmid, B., Petchey, O.L., Hueni, A., Schimel, D.S., Schaepman, M.E., 2017. Mapping functional diversity from remotely sensed morphological and physiological forest traits. Nat. Commun. 8, 1441. https://doi.org/10.1038/s41467-017-01530-3.

SEEA-EA, 2024. System of Environmental-Economic Accounting - Ecosystem Accounting (No. 124). Food and Agriculture Organization of the United Nations. https://seea.un.org/sites/seea.un.org/files/documents/EA/seea_ea_f124_web_12dec24.pdf.

Skidmore, A.K., Coops, N.C., Neinavaz, E., Ali, A., Schaepman, M.E., Paganini, M., Kissling, W.D., Vihervaara, P., Darvishzadeh, R., Feilhauer, H., Fernandez, M., Fernández, N., Gorelick, N., Geijzendorffer, I., Heiden, U., Heurich, M., Hobern, D., Holzwarth, S., Muller-Karger, F.E., Van De Kerchove, R., Lausch, A., Leitão, P.J., Lock, M.C., Mücher, C.A., O'Connor, B., Rocchini, D., Turner, W., Vis, J.K., Wang, T., Wegmann, M., Wingate, V., 2021. Priority list of biodiversity metrics to observe from space. Nat. Ecol. Evol. 5, 896–906. https://doi.org/10.1038/s41559-021-01451-x.

Tehrany, M.S., Kumar, L., Drielsma, M.J., 2017. Review of native vegetation condition assessment concepts, methods and future trends. J. Nat. Conserv. 40, 12–23. https://doi.org/10.1016/j.jnc.2017.08.004.

Tierney, G.L., Faber-Langendoen, D., Mitchell, B.R., Shriver, W.G., Gibbs, J.P., 2009. Monitoring and evaluating the ecological integrity of forest ecosystems. Front. Ecol. Environ. 7, 308–316. https://doi.org/10.1890/070176.

Valavi, R., Lehmann, E., Liu, N., Levick, S., Giljohann, K., Williams, K., Johnson, S., Botha, H., Munroe, S., Collings, S., Searle, R., Van Niel, T., Newnham, G., Paget, M., Joehnk, K., Hosack, G., Harwood, T., Malley, C., Gunawardana, D., Sivanandam, P., Richards, A., Tetreault Campbell, S., Ferrier, S., 2025. HCAS 3.1 (1988–2022) Base Model Estimate of Habitat Condition (90m grid) and National Connectivity Index (NCI) 2.0, Annual Epochs of HCAS from 1990 to 2022 for Continental Australia With Uncertainty. https://doi.org/10.25919/a3h3-bs84.

Venter, O., Sanderson, E.W., Magrach, A., Allan, J.R., Beher, J., Jones, K.R., Possingham, H.P., Laurance, W.F., Wood, P., Fekete, B.M., Levy, M.A., Watson, J.E.M., 2016. Global terrestrial human footprint maps for 1993 and 2009. Sci. Data 3, 160067. https://doi.org/10.1038/sdata.2016.67.

Venter, Z.S., Barton, D.N., Chakraborty, T., Simensen, T., Singh, G., 2022. Global 10 m land use land cover datasets: a comparison of dynamic world, world cover and Esri land cover. Remote Sens. 14, 4101. https://doi.org/10.3390/rs14164101.

Wang, Y., Zhang, Z., Feng, L., Ma, Y., Du, Q., 2021. A new attention-based CNN approach for crop mapping using time series Sentinel-2 images. Comput. Electron. Agric. 184, 106090. https://doi.org/10.1016/j.compag.2021.106090.

Watson, J.E.M., Jones, K.R., Fuller, R.A., Marco, M.D., Segan, D.B., Butchart, S.H.M., Allan, J.R., McDonald-Madden, E., Venter, O., 2016. Persistent disparities between recent rates of habitat conversion and protection and implications for future global conservation targets. Conserv. Lett. 9, 413–421. https://doi.org/10.1111/conl.12295.

White, M., Griffioen, P., Newell, G., 2020. Multi-temporal Land Cover and Native Vegetation Extent for Victoria (No. 311). Arthur Rylah Institute for Environmental Research. Department of Environment, Land, Water and Planning, Melbourne, Australia. https://www.environment.vic.gov.au/_data/assets/pdf_file/0042/479877/Victorian_Land_Cover_Time_Series_Data_1985-2019_DELWP_ARI_TechReport.pdf.

Williams, K.J., Ferrier, S., Lehmann, E.A., Harwood, T.D., Donohue, R.J., Giljohann, K.M., Valavi, R., Liu, N., Ware, C., Lyon, P., Niel, T.G.V., McVicar, T.R., Richards, A., Malley, C., 2024. Overcoming key challenges of satellite-based monitoring of ecosystem condition: a continental-scale example from Australia. In: EcoEvoRxiv Preprints.

Woodcock, R., Paget, M., Wang, P., Held, A., 2018. Accelerating industry innovation using the open data cube in Australia. In: IGARSS 2018–2018 IEEE International Geoscience and Remote Sensing Symposium, pp. 8636–8638. https://doi.org/10.1109/IGARSS.2018.8519170.

Wulder, M.A., White, J.C., Loveland, T.R., Woodcock, C.E., Belward, A.S., Cohen, W.B., Fosnight, E.A., Shaw, J., Masek, J.G., Roy, D.P., 2016. The global Landsat archive: status, consolidation, and direction. Remote Sens. Environ. 185, 271–283. https://doi.org/10.1016/j.rse.2015.11.032.

Wurtzebach, Z., Schultz, C., 2016. Measuring ecological integrity: history, practical applications, and research opportunities. BioScience 66, 446–457. https://doi.org/10.1093/biosci/biw037.

Xie, X., He, B., Guo, L., Miao, C., Zhang, Y., 2019. Detecting hotspots of interactions between vegetation greenness and terrestrial water storage using satellite observations. Remote Sens. Environ. 231, 111259. https://doi.org/10.1016/j.rse.2019.111259.

Yang, J., Guo, Y., Owers, C.J., Giljohann, K., Valavi, R., Donohue, R., Williams, K.J., Ferrier, S., Mokany, K., 2025. A framework for dynamic assessment of terrestrial ecosystem condition. Glob. Ecol. Biogeogr. 34, e70132. https://doi.org/10.1111/geb.70132.

Yen, J.D.L., Dorrough, J., Oliver, I., Somerville, M., McNellie, M.J., Watson, C.J., Vesk, P.A., 2019. Modeling biodiversity benchmarks in variable environments. Ecol. Appl. 29, 1–16. https://doi.org/10.1002/eap.1970.

Zhang, X., Zhou, Y., Luo, J., 2021. Deep learning for processing and analysis of remote sensing big data : a technical review. Big Earth Data 00, 1–34. https://doi.org/10.1080/20964471.2021.1964879.

Zhao, M., Zhou, Y., Li, Xuecao, Cao, W., He, C., Yu, B., Li, Xi, Elvidge, C.D., Cheng, W., Zhou, C., 2019. Applications of satellite remote sensing of nighttime light observations: advances, challenges, and perspectives. Remote Sens. 11, 1971. https://doi.org/10.3390/rs11171971.

Zhu, Z., Woodcock, C.E., 2012. Object-based cloud and cloud shadow detection in Landsat imagery. Remote Sens. Environ. 118, 83–94. https://doi.org/10.1016/j.rse.2011.10.028.

Zhu, X.X., Tuia, D., Mou, L., Xia, G.-S., Zhang, L., Xu, F., Fraundorfer, F., 2017. Deep learning in remote sensing: a comprehensive review and list of resources. IEEE Geosci. Remote Sens. Magaz. 5, 8–36. https://doi.org/10.1109/MGRS.2017.2762307.

Zhu, L., Webb, G.I., Yebra, M., Scortechini, G., Miller, L., Petitjean, F., 2021. Live fuel moisture content estimation from MODIS: a deep learning approach. ISPRS J. Photogramm. Remote Sens. 179, 81–91. https://doi.org/10.1016/j.isprsjprs.2021.07.010.